JVI Journals.ASM.org

Analysis of Serine Codon Conservation Reveals Diverse Phenotypic Constraints on Hepatitis C Virus Glycoprotein Evolution

Richard J. P. Brown,[a] George Koutsoudakis,[b] Richard A. Urbanowicz,[c,d] Deeman Mirza,[c,d] Corinne Ginkel,[a] Nina Riebesehl,[a] Noémie Calland,[e] Anna Albecka,[e] Louisa Price,[c,d] Natalia Hudson,[c,d] Véronique Descamps,[f] Matthijs Backx,[c,d] C. Patrick McClure,[c,d] Gilles Duverlie,[f] Eve-Isabelle Pecheur,[g] Jean Dubuisson,[e] Sofia Perez-del-Pulgar,[h] Xavier Forns,[h] Eike Steinmann,[a] Alexander W. Tarr,[c,d] Thomas Pietschmann,[a] Jonathan K. Ball[c,d]

Division of Experimental Virology, Twincore, Centre for Experimental and Clinical Infection Research, a joint venture between Medical School Hannover and Helmholtz Centre for Infection Research, Hannover, Germany[a]; Parc de Recerca Biomèdica de Barcelona, Department of Experimental and Health Sciences, Universitat Pompeu Fabra, Barcelona, Spain[b]; School of Life Sciences[c] and Nottingham Digestive Diseases Centre Biomedical Research Unit,[d] The University of Nottingham, Queen's Medical Centre, Nottingham, United Kingdom; Center for Infection & Immunity of Lille, INSERM U1019—CNRS UMR8204, Université Lille Nord de France, Institut Pasteur de Lille, Lille, France[e]; Laboratoire de Virologie EA4294, Centre Hospitalier Universitaire d'Amiens, Université de Picardie Jules Verne, Amiens, France[f]; UMR INSERM 1052/CNRS 5286, Centre de Recherche en Cancérologie de Lyon, Lyon, France[g]; Liver Unit, Hospital Clinic, IDIBAPS, CIBERehd, Barcelona, Spain[h]

Serine is encoded by two divergent codon types, UCN and AGY, which are not interchangeable by a single nucleotide substitution. Switching between codon types therefore occurs via intermediates (threonine or cysteine) or via simultaneous tandem substitutions. Hepatitis C virus (HCV) chronically infects 2 to 3% of the global population. The highly variable glycoproteins E1 and E2 decorate the surface of the viral envelope, facilitate cellular entry, and are targets for host immunity. Comparative sequence analysis of globally sampled *E1E2* genes, coupled with phylogenetic analysis, reveals the signatures of multiple archaic codon-switching events at seven highly conserved serine residues. Limited detection of intermediate phenotypes indicates that associated fitness costs restrict their fixation in divergent HCV lineages. Mutational pathways underlying codon switching were probed via reverse genetics, assessing glycoprotein functionality using multiple *in vitro* systems. These data demonstrate selection against intermediate phenotypes can act at the structural/functional level, with some intermediates displaying impaired virion assembly and/or decreased capacity for target cell entry. These effects act in residue/isolate-specific manner. Selection against intermediates is also provided by humoral targeting, with some intermediates exhibiting increased epitope exposure and enhanced neutralization sensitivity, despite maintaining a capacity for target cell entry. Thus, purifying selection against intermediates limits their frequencies in globally sampled strains, with divergent functional constraints at the protein level restricting the fixation of deleterious mutations. Overall our study provides an experimental framework for identification of barriers limiting viral substitutional evolution and indicates that serine codon-switching represents a genomic "fossil record" of historical purifying selection against E1E2 intermediate phenotypes.

Hepatitis C virus (HCV) is an enveloped, positive-strand RNA virus and causes a significant disease burden worldwide (1). A chronic infection ensues in around 80% of cases, predisposing carriers to an increased risk of cirrhosis and hepatocellular carcinoma (2). HCV exhibits substantial genetic diversity globally, with six well-sampled genotypes and a multitude of subtypes having been described (3). This observed genetic heterogeneity results from a high mutation/replicative rate *in vivo* (4, 5) and extends to the intrahost level, where the virus exists as an ensemble of genetically related yet distinct variants (6, 7). However, this genetic heterogeneity is not evenly distributed throughout the viral genome. The greatest levels of diversity are observed in the *E1E2* genes, encoding the envelope glycoproteins E1 and E2, heterodimers of which are distributed over the surface of the viral lipid envelope. Genotype-specific positive selection, mediated by humoral and cellular targeting, contributes to global *E1E2* evolution (8). Progressive substitutional evolution of the *E1E2* genes, in part facilitated by immunological targeting of the envelope glycoproteins, contributes to the generation of intrahost viral complexity (9–12). Indeed, neutralizing antibody targeting of E1E2 selects for functional escape mutants from the pool of genetic variants within an infected host (13, 14). However, *E1E2* sequence change is also restricted by structural and functional constraints associated with virion assembly (15–17), correct folding (18), direct interaction with the cellular receptors CD81 (19) and SR-BI (20), undefined interactions with additional essential entry cofactors (21, 22), and determinants associated with membrane fusion (23, 24).

Serine is unique among amino acids: it is encoded by two divergent codon types (UCN and AGY) which are not interchangeable by a single-nucleotide substitution. S-S codon switching at conserved serine residues via simultaneous double-nucleotide substitutions (UC to AG) has been observed in conserved eukaryotic and prokaryotic proteins (25). Substitution via this mechanism is synonymous and selectively neutral. S-S switching could also arise via two temporally spaced single-nucleotide substitutions (UC to AC to AG, or UC to UG to AG) requiring an intermediate phenotype encoding threonine (T) or cysteine (C). Sub-

Received 27 June 2013 **Accepted** 23 October 2013
Published ahead of print 30 October 2013
Address correspondence to Richard J. P. Brown, richard.brown@twincore.de, or Jonathan K. Ball, jonathan.ball@nottingham.ac.uk.

doi:10.1128/JVI.01745-13
The authors have paid a fee to allow immediate free access to this article.

stitution via this mechanism is likely due to a transient period of relaxed purifying selection. The paradigm of S-S codon switching in the context of *E1E2* evolution represents a rare biological phenomenon which can be utilized to investigate the fluctuating fitness landscapes, including restrictions on genome mutability, which shape RNA virus evolution. Indeed, HCV represents an ideal model pathogen for such investigations due to its global dissemination, high levels of sequence divergence, and good representation in sequence databases, in addition to an array of well-characterized *in vitro* systems allowing mechanistic dissection of multiple aspects of the viral life cycle. Our analyses indicate that fixed S-S switches in HCV genotypes/subtypes are archaic and represent the genomic scars of former selection against less-fit intermediate phenotypes at the host-virus interface. Together these data reveal the dynamic mutational processes which underlie apparently conserved residues and shape global patterns of viral sequence divergence.

MATERIALS AND METHODS

Database searching and sequence alignment. All available full-length *E1E2* sequences from the LANL, DDJB, and EU-HCV HCV databases were initially downloaded. To achieve a data set representative of globally sampled HCV *E1E2* diversity and reduce numerical bias toward genotypes/subtypes which predominate in developed nations, a manual iterative selection procedure was employed. Multiple sequences derived from the same patient, in addition to epidemiologically linked and highly related viral strains, were sequentially removed. A final data set of 170 *E1E2* genes was utilized to assess levels of S-S switching in HCV genotypes 1 to 6 sampled worldwide. *E1E2* sequences were aligned according to overlying amino acids using MEGA5 (26). Indels and regions of ambiguous alignment were gap stripped. Codon types and frequencies at conserved residues were counted manually.

Phylogenetic analysis. A maximum likelihood phylogeny was generated using the GTR+I+Γ_4 model in PhyML 3.0 (27). S-S codon switches were mapped onto the internal branches of the phylogeny according to the parsimony criterion.

Generation of transitional mutant panels. JFH-1 E1E2 (amino acids [aa] 170 to 746) mutants were generated in plasmid phCMV using a QuikChange II site-directed mutagenesis kit (Agilent Technologies). An identical mutant panel was generated in plasmid pJFH-1 (28), containing a full-length genotype 2 genome, as previously described (18). A subset of mutations were additionally cloned into the H77/JFH-1 full-length chimeric genome. All mutations were confirmed by sequencing.

GNA capture and conformational detection of serine mutants. E1E2s were transiently expressed in HEK 293FT cells. E1E2 expression in cellular lysates was confirmed by Western blotting with monoclonal antibody (MAb) AP33, while total expressed protein was quantified via titration curves using MAb AP33. Microtiter plates (Nunc Maxisorp) were coated with 5 μg/ml *Galanthus nivalis* agglutinin (GNA; Sigma) and incubated overnight at 4°C. Wells were blocked with 5% milk–phosphate-buffered saline (PBS)–Tween for 2 h before the addition of 4-fold-diluted proteins in PBS and incubated at room temperature for 2 h. Plates were washed three times with 0.05% PBS-Tween, and proteins were detected with MAbs AP33, ALP98, 1:7, AR3A, AR3B, AR3C, and CBH4G at a concentration of 1 μg/ml. Horseradish peroxidase (HRP)-conjugated anti-mouse or anti-human antibodies (Sigma) in 0.05% PBS-Tween (1/1,000 dilution) were used to detect the primary antibodies after incubation 1 h at room temperature. After washing, *p*-nitrophenyl phosphate (pNPP; Sigma) substrate was added, and the reaction was stopped with 1 M H_2SO_4. Plates were developed and read at 405 nm (Molecular Devices V max plate reader). Antibody binding was normalized to total protein expression, as determined by reactivity to MAb ALP98, and is presented relative to the value for wild-type (WT) JFH-1 (100%).

HCV pseudoparticle production. HCV pseudoparticles (HCVpps) were generated as previously described (29). Plasmid ΔE1E2 phCMV was used as a negative control. After 72 h, supernatants containing pseudoparticles were filtered through a 0.45-μm-pore-size membrane and used to infect Huh7 cells. The infectivity of HCVpps on target Huh7 cells was assessed after 48 h using a firefly luciferase reporter gene activity kit (Promega) according to the manufacturer's protocol.

Western blotting and CD81 pulldown assays. HEK 293T cells producing HCVpps were lysed with 1% Triton X-100. For CD81 pull-downs, recombinant fusion proteins containing the large extracellular loop of CD81 fused to glutathione *S*-transferase (GST) were preadsorbed onto glutathione-Sepharose beads (Pharmacia Biotech) and incubated with lysates of HCVpp-producing cells or supernatants containing ultracentrifuged HCVpps. After overnight incubation, beads were washed with lysis buffer. After separation by SDS-PAGE, proteins were transferred to nitrocellulose membranes (Hybond-ECL; Amersham) using a Trans-Blot apparatus (Bio-Rad). Separate detection of E1, E2, and retroviral Gag was achieved using MAbs 1C4 (anti-E1; 1/100) (Innogenetics), 3/11 (anti-E2; 1/2000) (30), and R187 (ATTC CRL1912) (anti-Gag; 1/500), respectively, followed by secondary detection with HRP-conjugated immunoglobulin and visualization by enhanced chemiluminescence detection (ECL; Amersham) as recommended by the manufacturer.

HCV cell culture (HCVcc) virus production. RNA transcription, electroporation, and anti-NS5A antigen detection via immunofluorescence microscopy were performed as previously described (28, 31). Transfected cells and supernatants were harvested at 72 h postelectroporation to determine intracellular and extracellular levels of infectious particles and core antigen. A replication-deficient NS5B ΔGDD mutant and the assembly-impaired partialΔE1E2 mutant were included as controls.

Isolation of intracellular viral fractions. Lysates containing intracellular viral fractions were isolated from transfected Huh7.5 cells at 72 h postelectroporation by repeated freeze-thawing cycles in liquid nitrogen (17).

Determination of titers of infectious particles. Viral titers were determined via limiting dilution assays and anti-NS5A staining at 72 h postelectroporation. The 50% tissue culture infective doses ($TCID_{50}$) and numbers of focus-forming units (FFU) for each electroporation were calculated using the method of Reed and Muench (32).

HCVcc core quantification assay. Huh7.5 cells containing replicating virus were harvested at 72 h postelectroporation, washed three times in PBS, and lysed via the addition of 1% Triton X in PBS. Intracellular lysates were subsequently diluted 1:500 in 1% Triton X-100 in PBS. HCVcc supernatants were collected 72 h postelectroporation and diluted 1:5 in 1% Triton X-100 in PBS. Core was quantified by an automated chemiluminescent microparticle immunoassay (Architect HCVAg, Abbott, Germany).

Membrane fusion assay. Supernatants containing WT JFH-1, in addition to assembly/entry-deficient mutants, were normalized to the total amount of core and concentrated by centrifugation through a 20% sucrose cushion for 4 h at 4°C and 32,000 rpm. Concentrated pellets were resuspended in 150 mM NaCl, 10 mM Tricine-NaOH (pH 7.4). Liposomes were prepared by extrusion as previously described (24), from phosphatidylcholine-cholesterol-octadecyl rhodamine B chloride (PC-chol-R_{18}) in a 65:30:5 molar ratio (final lipid concentration, 5 mM). The lipid mixing assay between HCVcc and liposomes was based upon R_{18} dequenching and was performed as previously described (23). Fusion kinetics were recorded using a dual-channel PicoFluor fluorimeter (Turner Biosystems, Sunnyvale, CA). Maximal R_{18} dequenching was measured after the addition of 0.1% Triton X-100 to the cuvette. Experiments were performed in triplicate.

Infectious-particle neutralizations. Single-point HCVcc neutralizations were performed in triplicate by incubation at 37°C for 1 h of 100 FFU and 200 FFU WT JFH-1, plus each mutant virus, with 10 μg/ml MAb 1:7. After incubation, virus/MAb mixtures were added to uninfected Huh7.5 target cells in a 96-well plate (1.5×10^4 cells/well) and incubated at 37°C

for 4 h and then replaced with 200 μl Dulbecco's modified Eagle medium (DMEM). For control purposes, 100 FFU and 200 FFU of WT JFH-1, plus each mutant, minus MAb 1:7, were added to uninfected Huh7.5 target cells as described above. Cells were incubated for a total of 72 h postinfection and stained for NS5A. Foci were counted manually.

Statistical analyses. All statistical analyses were performed using GraphPad Prism 6 software.

RESULTS

Quantification of global HCV E1E2 S-S switching at conserved residues. Inspection of translated *E1E2* genes revealed nine highly conserved serine residues (Fig. 1A, top). Residues S198, S211, S307, S419, and S432 were associated with conserved NXS potential N-linked glycosylation (PNG) sites. Analysis of underlying codon structures revealed the signatures of S-S codon switching (UCN to AGY or AGY to UCN) at residues S198, S211, S327, S419, S432, S512, and S686, detectable at both the inter- and intragenotypic levels (Fig. 1A, bottom). Two serine residues where no switching was evident (S273 and S307) were identified in E1. Threonine intermediates were observed at low levels at residues S198, S432, and S686. No cysteine intermediates were observed at any position.

Frequencies of each serine codon type, in addition to frequencies of threonine intermediates (ACN), were calculated for each conserved residue on a genotype-specific basis (Fig. 1B). Additionally, residue 243 was also included in the analyses, representing a less conserved control residue (Con243) which can accommodate sequence changes more readily, for use in downstream phenotypic investigations. Threonine intermediates were apparent at low frequencies in genotype 1 (T198, 18.5%; T432, 3.7%; T686, 18.5%) and genotype 6 (T198, 2.1%; T432, 2.1%; T686, 2.1%) E1E2s. Additionally, low-frequency threonine intermediates, plus both serine codon types, were observed in genotype 6 viruses at residue S198 and genotype 1 and 6 viruses at residue S432. Together these data indicate that serine codon switching in globally sampled HCV glycoproteins can proceed through threonine intermediates but not cysteine. However, the low frequencies and limited distribution of threonine intermediates at conserved serine residues indicate that their occurrence is restricted or transient.

Mapping S-S codon switches onto the E1E2 phylogeny. S-S codon switches were mapped onto the branches of the HCV E1E2 phylogeny according to the parsimony criterion. A total of 16 codon switches were detected: 11 AGY-to-UCN switches and five UCN-to-AGY switches (Fig. 2). All S-S switches occurred on internal branches, leading to genotype/subtype-specific clades, and had become fixed in particular genotypes/subtypes. Only a single S-S codon switching event was detected on a terminal branch in the genotype 2 clade. Together, these data indicate that the majority of S-S codon switches in *E1E2* are archaic, appearing in the deeper portions of HCV phylogeny. If these deep S-S switches proceeded through threonine intermediates, the genetic signatures were no longer detectable in extant circulating viruses.

Low-frequency threonine intermediates were also mapped on the *E1E2* phylogeny and were generally located sporadically on terminal branches and detected only in genotype 1 and 6 viruses at residues 198, 432, and 686. No threonine intermediates had become fixed in any particular genotype/subtype. However, T198 ($n = 5$) and T686 ($n = 5$) intermediates had become fixed, to some degree, in two distinct subsets of genotype 1a strains. Together, these data indicate that threonine residues are rare and detectable only on terminal branches or in the more recent portions of the E1E2 phylogeny, indicating that the observed threonine residues are transient, possibly possessing selectively deleterious phenotypes.

Rationale behind generation of intermediate phenotype panel. Threonine mutants (S to T) were investigated for their effects on E1E2 phenotype, at a total of 10 positions (Fig. 1). No cysteine intermediates were detected in our codon usage pattern analyses of global isolates (Fig. 1 and 2). Additionally S-to-C mutations at positions 198, 211, 307, 327, 419, and 432 would disrupt conserved PNG sites which have been demonstrated to play an essential role in E1E2 function (18, 33, 34). Consequently, S-to-C mutations which were not associated with conserved PNG sites (E1 S273C and E2 S512C) were generated at two positions for control purposes.

Substitution of conserved serine residues with threonine frequently results in enhanced epitope exposure. E2 glycoprotein expression and protein fold were assessed by GNA capture enzyme-linked immunosorbent assay (ELISA) (Fig. 3A to F). All expressed proteins were recognized by MAb AP33 (Fig. 3A), and all except the S512C mutant were recognized by MAbs targeting conformational epitopes (Fig. 3B to F). Thus, all mutant E2 glycoproteins except the S512C mutant are likely to be correctly folded. Importantly, many S-to-T mutants exhibited recognition by specific antibodies that was significantly enhanced compared to that of WT JFH-1, presumably due to increased epitope exposure (Fig. 3A to F). Unfortunately, due to the lack of a suitable E1-specfic conformational antibody, we were unable to assess the fold of E1. However, interestingly, mutations in E1 can result in enhanced recognition by MAbs targeting E2 (Fig. 3A to F).

Heterodimerization and CD81 binding were assessed by Western blotting and subsequent CD81 pulldowns (Fig. 3G). A robust E1 and E2 signal was detected for all mutant lysates, indicating that intermediate phenotypes have no deleterious effect on E1E2 heterodimerization. In the CD81 pulldown assay, a reduced signal was observed for both E1 and E2 for the S419T and S512C mutants, indicating that these mutations affect the CD81 binding ability of the expressed proteins.

Transitional mutants confer a diverse range of infectivities to retroviral pseudoparticles. The S198T, S243T, S432T, and S512T mutant HCVpps were able to infect target cells with consistently increased efficiency compared to WT JFH-1 E1E2, presumably due to increased exposure of receptor binding sites (Fig. 4A). In contrast, the S211T, S273T, S273C, S419T, S512C, and S686T mutants exhibited a significant reduction in their capacity to infect permissive cells. Of note, both the S273C and S512C proteins caused a highly significant ($P < 0.0001$) reduction in infectivity (<10% of that of WT JFH-1). Together, these data indicate that transitional phenotypes can have differential effects on envelope glycoprotein entry fitness *in vitro*: a proportion of S-to-T mutations confer increased capacity for efficient target cell entry in the HCVpp system, while others significantly reduce efficient entry. S-to-C intermediate phenotypes appear to result in highly entry-deficient HCVpps.

Mutant E1E2 heterodimerization and incorporation into purified HCVpp preparations were assessed via Western blotting, with subsequent CD81 pulldowns to assess receptor binding (Fig. 4B). Comparable levels of retroviral Gag were detected for all preparations, indicating that transitional phenotypes have no del-

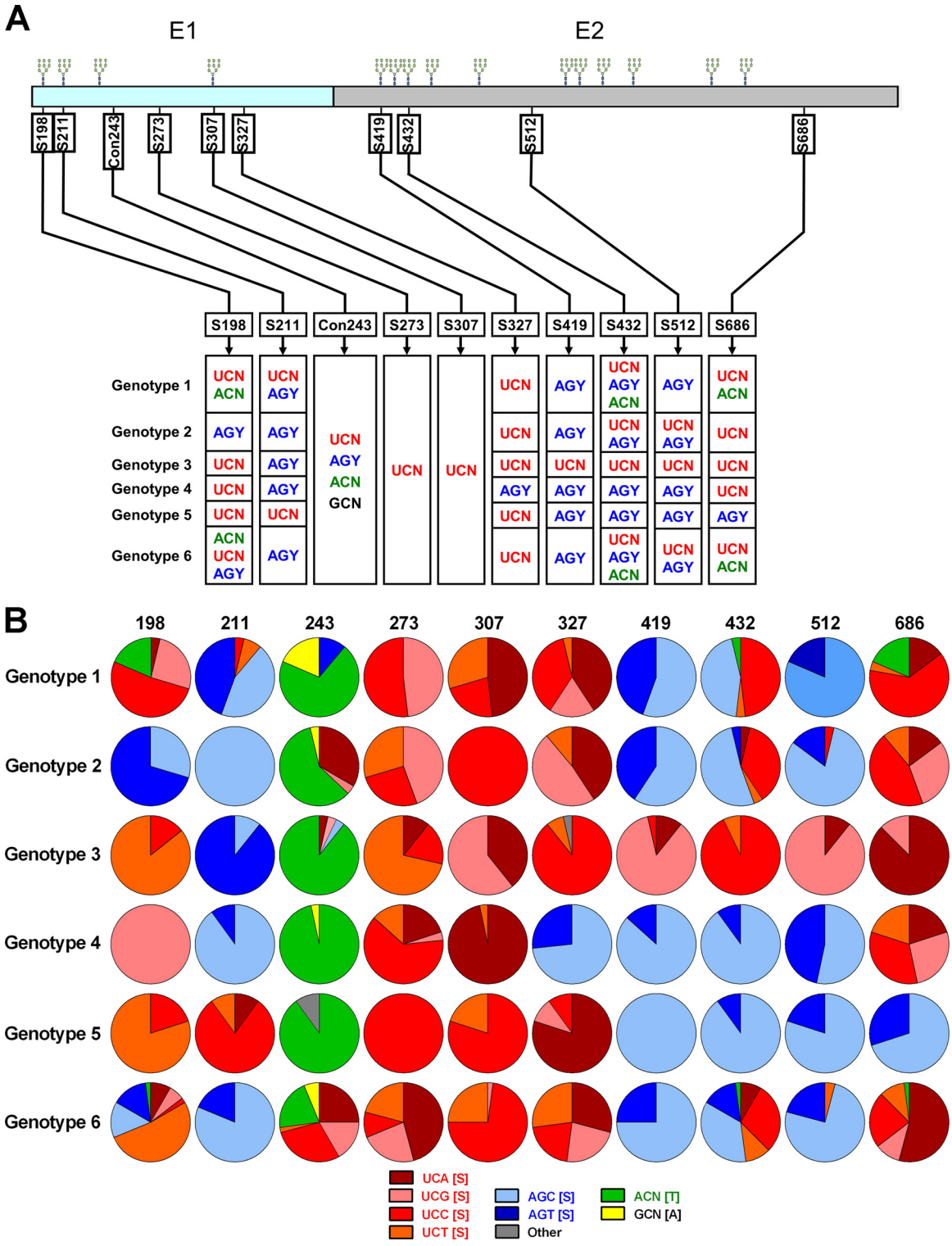

FIG 1 Location and codon structure of conserved E1E2 serines. (A) Schematic depicting locations of conserved nine serine residues in HCV E1E2. Positions of conserved glycans are indicated above the E1E2 protein, while coordinates of the nine serine residues are beneath it and are numbered relative to homologous positions in the H77 reference strain (NC_004102) (top). Codon structures for each conserved serine residue are presented as columns and are segregated according to HCV genotype (bottom). Con243 is a control residue which was included for downstream reverse genetics experiments. (B) Genotype-specific codon usage patterns are presented as pie charts and are segregated according to HCV genotype.

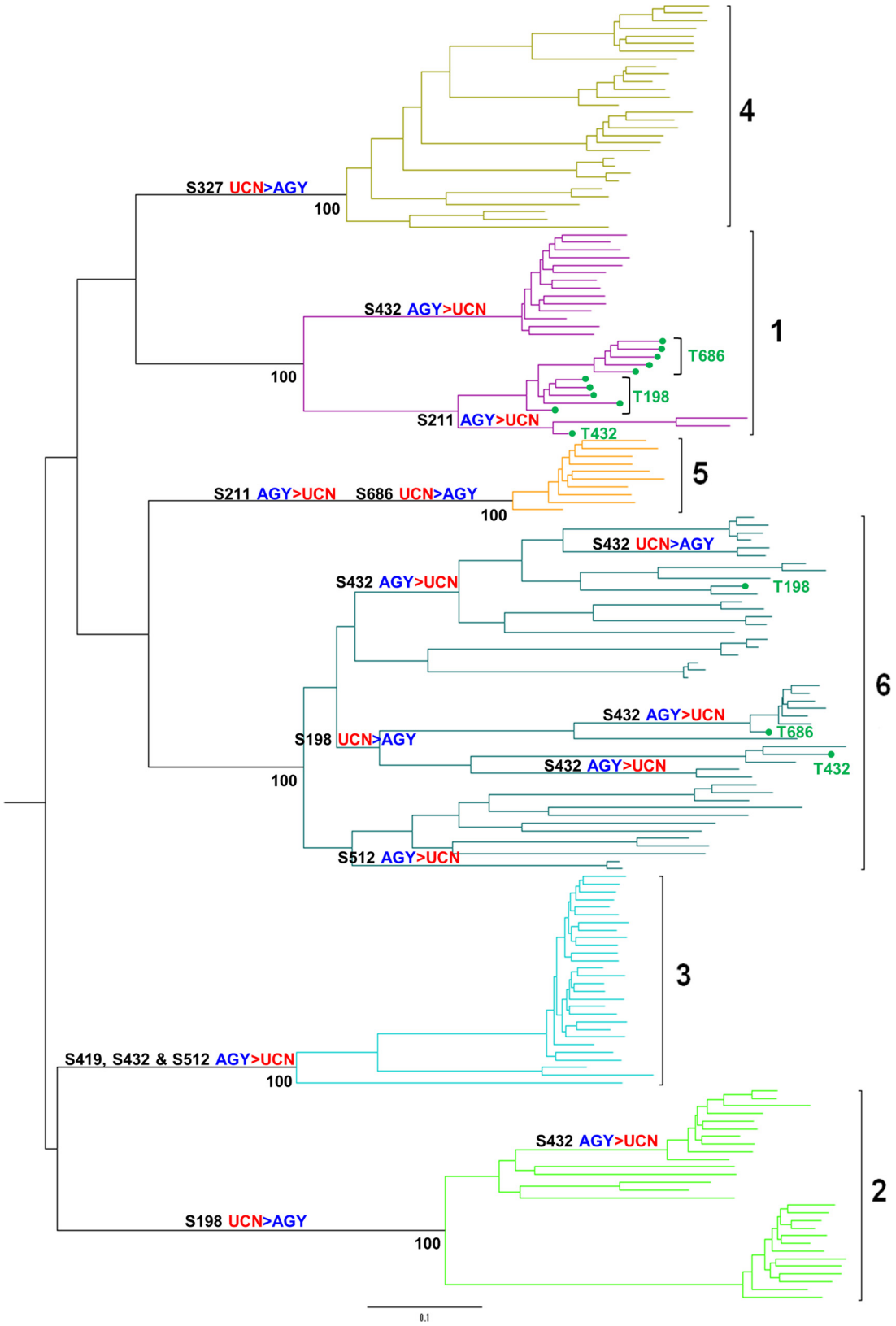

FIG 2 Mapping of serine codon switches onto the global HCV phylogeny. S-S switches were mapped onto internal branches of the *E1E2* phylogeny according to the parsimony criterion. The location and polarity of individual S-S switches are indicated above the branches on which they occur. Significant bootstrap values indicating the monophyly of the 6 major genotypes are located below internal nodes. Isolates which harbor threonine intermediates, and residues at which they are detected, are in green on terminal branches. Branch lengths are proportional to genetic distance.

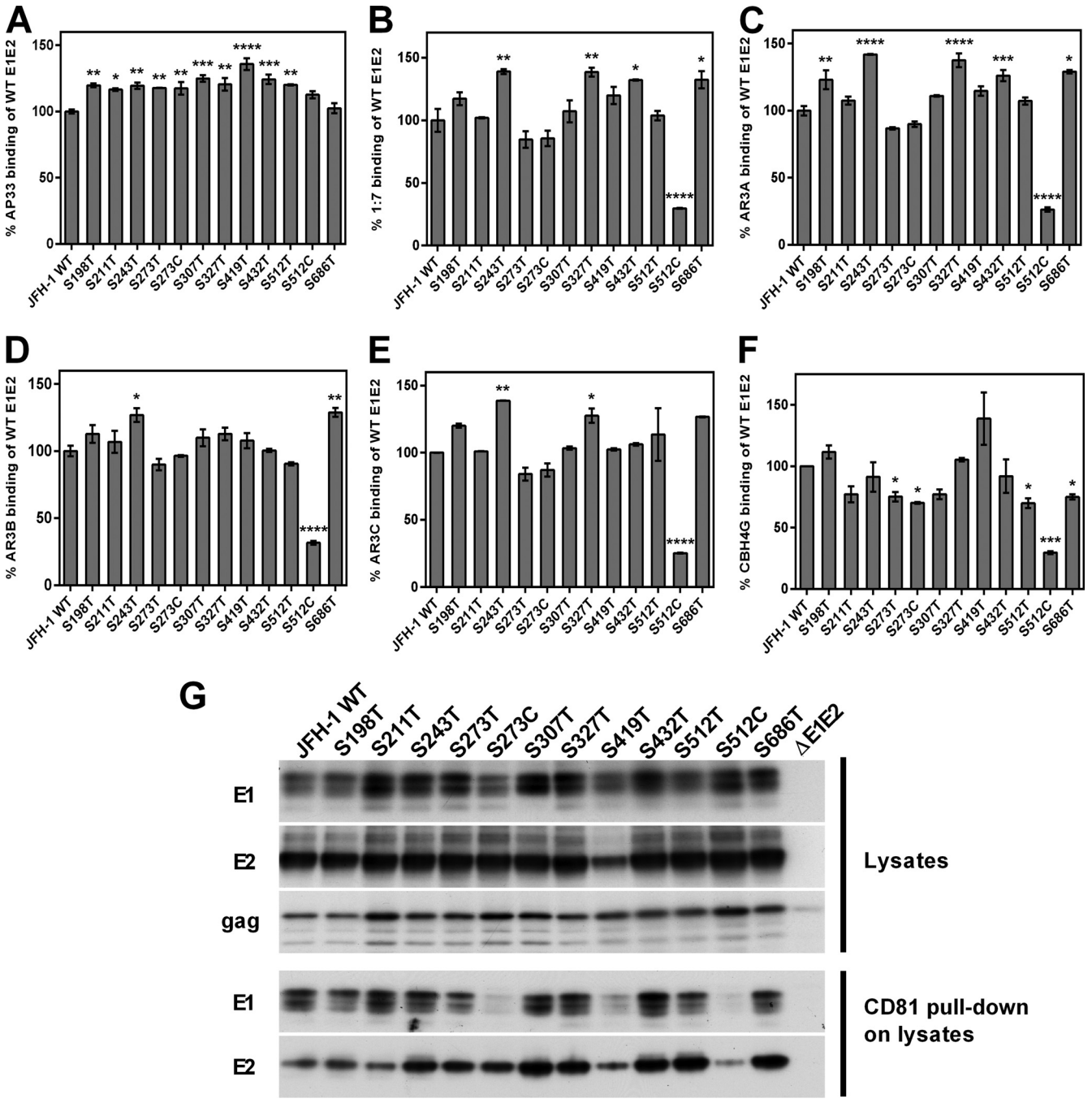

FIG 3 Conformation, epitope exposure, heterodimerization, and CD81 binding of transitional phenotypes. E1E2s present in cell lysates were captured by GNA and then probed with a panel of MAbs recognizing either linear (A) or conformation-sensitive (B to F) epitopes. Data were normalized for overall protein expression by GNA capture ELISA using MAb ALP98, and then binding was normalized to that observed for the WT JFH-1 E1E2 (100%). Values are means from at least two independent assays; error bars show standard errors of the means (SEM). MAbs used were AP33 (A), 1:7 (B), AR3A (C), AR3B (D), AR3C (E), and CBH4G (F). Statistical significance of differences in antibody recognition between individual mutants and WT JFH-1 were assessed by one-way analysis of variance (ANOVA) followed by Dunnett's multiple comparison test: *, $P < 0.05$; **, $P < 0.01$; ***, $P < 0.001$; ****, $P < 0.0001$. (G) For Western blotting of cell lysates, cell lysates were analyzed via Western blotting using MAbs 1C4, 3/11 and anti-GAG to detect E1, E2, and Gag, respectively. For CD81 pulldown of cell lysates, E1E2s were pulled down from lysates via CD81-LEL-GST immobilized onto Sepharose beads and analyzed via Western blotting. The MAbs 1C4 and 3/11 and were used to detect E1 and E2, respectively.

eterious effect on HCVpp release. An E1 and E2 signal was detected for all purified HCVpp preparations analyzed, indicating that mutant E1E2 glycoproteins were successfully incorporated into pseudoparticles. However, the relative levels of both E1 and E2 incorporation were reduced for the intermediate phenotypes S419T and S512C. Reduced signals were observed for S419T and S512C proteins in the CD81 pulldown assay, indicating that these mutations affect CD81 binding. Together these results suggest

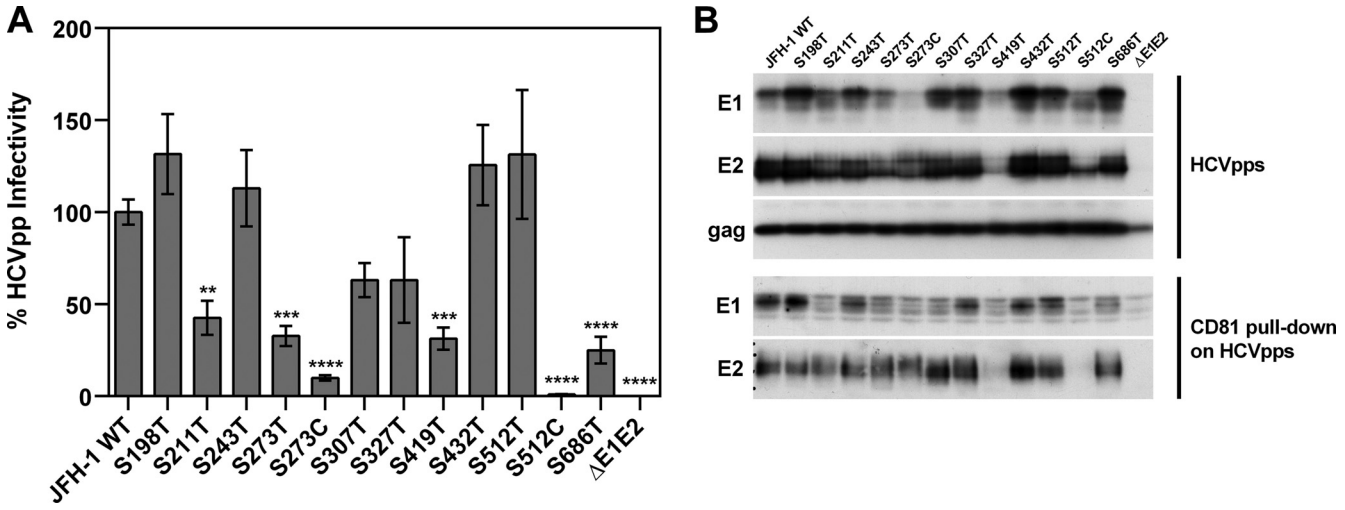

FIG 4 Infectivity, heterodimer incorporation and CD81 binding of retroviral pseudoparticles bearing transitional phenotypes. (A) HCVpp infectivity conferred by each mutant E1E2 normalized to WT JFH-1 E1E2 infectivity (100%). Infectivity assays were performed in triplicate; values are means from three independent experiments, and error bars show SEM. Statistical significance of differences in HCVpp infectivity between individual mutants and WT JFH-1 was assessed by one-way ANOVA followed by Dunnett's multiple comparison test: *, $P < 0.05$; **, $P < 0.01$; ***, $P < 0.001$; ****, $P < 0.0001$. (B) Supernatants containing HCVpps were analyzed by Western blotting after ultracentrifugation, using MAbs 1C4, 3/11, and R187 to detect E1, E2, and Gag, respectively. HCVpps were pulled down via CD81-LEL-GST immobilized on Sepharose beads and analyzed via Western blotting. MAbs 1C4 and 3/11 and were used to detect E1 and E2, respectively.

that transitional phenotypes have no deleterious effect on pseudoparticle release or heterodimer formation but can result in reduced heterodimer incorporation into HCVpps. Downstream, this can affect the ability to bind CD81.

Transitional phenotypes can result in both assembly- and entry-deficient authentic viral particles. The effect of intermediate phenotypes on viral replication and infectious particle production were investigated using the HCV cell culture (HCVcc) system (28, 31). Viral replication was assessed via immunofluorescence staining, with all intermediates displaying NS5A antigen expression comparable to that of WT JFH-1 (Fig. 5A). To assess the effect of intermediates on infectious virion production, intra- and extracellular titers of infectious particles were determined (Fig. 5B). No significant impact on the infectivity of intracellular fractions was observed compared to intracellular WT JFH-1, although intracellular titers were low (generally $<1 \times 10^3$ $TCID_{50}$/ml). While the S273T mutation resulted in a significant increase in the infectivity of extracellular virions compared to WT JFH-1, both S512C and S686T mutations resulted in a significant (>2-log) reduction in infectivity of secreted virions. Parallel (although nonsignificant) reductions in the infectivity of the intracellular fraction indicate that neither of these mutations results in viral egress defects.

Quantitative anti-core ELISA was performed on intra- and extracellular viral fractions derived from mutants which displayed significantly enhanced or reduced extracellular infectivity (Fig. 5). S273T mutations did not result in secretion of significantly more core than WT JFH-1, indicating that this mutation confers an enhanced capacity to enter permissive cells, rather than increased infectious particle production. Despite a significant ($P < 0.001$) reduction in secreted core, both intra- and extracellular core amounts for S686T mutants (582,590 and 10,269 fmol/liter) were comparable to those obtained with WT JFH-1 (426,428 and 17,368 fmol/liter), indicating that this intermediate confers a fitness cost at both the assembly and entry steps of the viral life cycle. Contrastingly, S512C mutants resulted in a highly significant ($P < 0.0001$) reduction in secreted core (2,924 fmol/liter) compared to WT JFH-1. Indeed, S512C mutants possessed an infectivity and core release profile that is nearly identical to that of the assembly-impaired ΔpartialE1E2 control mutant (2,284 fmol/liter) (16, 28) (Fig. 5B and C), indicating that S512C possesses an assembly-impaired phenotype. Together these data demonstrate that intermediates can result in glycoproteins that are defective for efficient virion assembly and target cell entry and indicate that global selection against phenotypic intermediates can act at the level of virion assembly and entry. Additionally, these data suggest that, in certain instances, the HCVpp system can be a poor predictor of E1E2 function. Indeed, a subset of mutations that conferred entry-impaired phenotypes in the HCVpp system were highly competent for entry in the HCVcc system.

Additionally, supernatants from entry/assembly-defective authentic viral particles were assessed for their capacity to mediate membrane fusion as previously described (23) (Fig. 5D). WT JFH-1 virions displayed pH-dependent, CD81-independent lipid mixing activity with R_{18}-labeled liposomes. Interestingly, S686T mutant viruses displayed mildly enhanced fusion activity compared to WT JFH-1, demonstrating that this mutation mediates its refractive effect at some other step in the entry cascade. Despite addition of equivalent amounts of the S512C mutant, normalized to extracellular core, supernatants derived from S512C mutants displayed negligible fusion activity, indicating that this mutation negatively impacts multiple stages in the entry process.

Phenotypes of transitional mutations are determined by genetic background. To test whether the phenotype of intermediates was determined by genetic background, a subset of S-to-T mutations were cloned in to the chimeric H77/JFH-1 genome, which contains the structural proteins from a genotype 1a virus. Intermediate phenotypes exhibited no negative effect on viral replication compared to H77 WT control (Fig. 6A). A significant

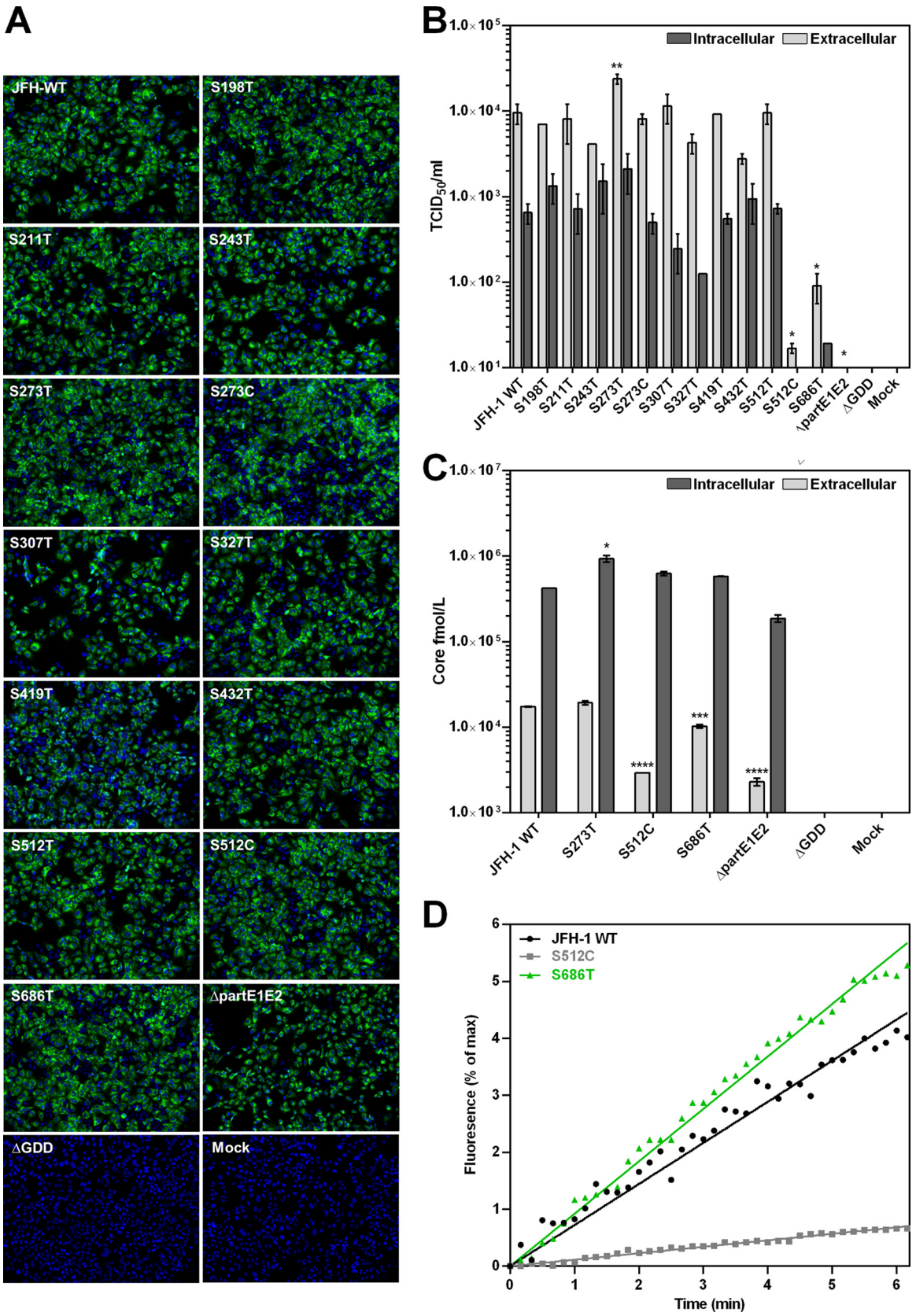

reduction in both intra- and extracellular infectivity was observed for S327T and S419T mutants, while the S686T intermediate had no discernible impact on the infectivity of intra- and extracellular fractions (Fig. 6B). These data contrast starkly with those obtained for these mutations in the Gt2a JFH-1 background. Again, the dual infectivity decrease observed for intra- and extracellular fractions for S327T and S419T suggests that neither of these mutations affects particle release. Quantitative anti-core ELISA indicated that intra- and extracellular levels of core for the S327T transitional mutant were comparable to those for WT H77, indicating that the S327T mutant is entry defective and not compromised at the level of assembly (Fig. 6C). Contrastingly, a significant reduction in the amount of secreted core observed for S419T mutants indicates that this intermediate confers a fitness cost at both the assembly and entry steps of the viral life cycle. Together these data indicate that the entry/assembly phenotype of transitional intermediates is genotype specific and modulated by genetic background.

Restriction against transitional phenotypes can be mediated by immunological targeting. To investigate whether transitional phenotypes, which were not compromised for entry or assembly, rendered E1E2s more susceptible to immunological targeting, antibody neutralization experiments were performed using human anti-E2 MAb 1:7 (35) (Fig. 7). Importantly, authentic virions bearing S327T mutations were rendered highly susceptible to 1:7 neutralization. Recently, mutations in E1 were shown to render viruses more sensitive to inhibition by soluble CD81 (36). Similarly, our data suggest that conservative S-to-T mutations in E1 can render HCV highly susceptible to antibodies targeting the discontinuous CD81 binding regions in E2. Additionally, these data provide proof of principle that restriction against transitional phenotypes can be mediated by host humoral targeting.

DISCUSSION

The absence of host humoral antagonism in the preseroconversion phase of acute HCV infection provides a temporary window for HCV to exploit previously deleterious mutational space and may facilitate serine codon switching via intermediates. Previously, we modeled HCV transmission and acute infection *in vivo*, infecting uPA/SCID chimeric mice with a defined source inoculum and identifying key glycoprotein determinants selected at transmission (37). Parallel selection of S198T mutations in independent transmission experiments provides supporting evidence that acute infection may provide a transient window facilitating serine codon switching via threonine intermediates (37). Reinstatement of immune pressure postseroconversion may render viruses that predominate in the absence of humoral targeting selectively deleterious, with humoral counteradaptive targeting of viral populations requiring reciprocal outgrowth of escape variants to ensure viral survival. Indeed, the virus must evolve to counter the constantly evolving B-cell repertoire, with anti-HCV MAbs derived from human combinatorial antibody libraries targeting multiple distinct antigenic regions (35, 38, 39) and conferring protection against experimental infection *in vivo* (40, 41). *In vitro* studies indicate that removal of specific PNG sites (18, 34) and deletion of HVR1 (42) render HCV more susceptible to antibody-mediated neutralization by unmasking neutralization-sensitive epitopes, although these artificial modifications do not occur naturally. In similar fashion, our data indicate that S-to-T substitutions, which are observed in naturally circulating viruses at low frequencies, can enhance epitope exposure to multiple MAbs targeting E2 in a residue-specific fashion (Fig. 3A to F). Additionally, the significantly increased sensitivity to neutralization conferred to genotype 2a authentic viral particles by one transitional phenotype (Fig. 7) provides proof of principle that intermediates can result in significantly reduced envelope glycoprotein fitness in the face of humoral immune pressure, while entry fitness is maintained. Together, these data suggest that a proportion of S-S codon conversions represent the genomic relics of reciprocal HCV counteradaptive mutational escape from host humoral targeting (43).

Deletion of partial E1E2 sequences (16, 28), intergenotypic domain swapping (15, 44), and mutations which abrogate glycoprotein heterodimerization (17, 45) can all result in assembly-impaired phenotypes. Additionally, our data identify mutations in both E1 and E2 which negatively impact efficient assembly of authentic virions bearing both genotype 1a and 2a glycoproteins. In the context of genotype 2a glycoproteins, the S512C transitional phenotype results in conformational disruption of E2, impaired CD81 binding, reduced heterodimer incorporation into HCVpps, and assembly-impaired authentic virions and abrogates pH-mediated membrane fusion. However, this effect is modulated by residue type, as S-to-T mutations at this position mediate no refractive effects. Unsurprisingly, these data suggest that structural restrictions against S-to-C intermediates are more extreme than those for S-to-T intermediates. These effects act in addition to previously reported constraints against non-S/T residues associated with PNG sites (18, 34). However, restriction against S-to-C intermediates is dependent on residue position, as S273C transitional phenotypes exert no deleterious effect on HCVcc entry, although HCVpps are entry defective. Together these data indicate that structural restrictions against fixation of S-to-C phenotypes are more pronounced than those for S-to-T phenotypes and are apparent at the level of virion assembly. Indeed, no detection of S-to-C intermediate phenotypes in globally sampled isolates is

FIG 5 Impact of transitional phenotypes at various stages of the viral life cycle. (A) Viral replication was assessed via anti-NS5A immunofluorescence staining with MAb 9E10 at 48 h postelectroporation. NS5A antigen (green) and nuclear counterstaining (blue) images were recorded separately and merged. (B) Titers of infectious particles in both intracellular and extracellular fractions were determined at 72 h postelectroporation via $TCID_{50}$. $TCID_{50}$ values are means from two independent experiments; error bars show SEM. (C) The amount of core antigen (fmol/liter) in both intracellular and extracellular fractions was determined at 72 h postelectroporation via anti-core ELISA. Core amounts presented are means from two independent experiments; error bars show SEM. Statistical significance of differences in both intracellular and extracellular HCVcc infectivity and amounts of core between individual mutants and WT JFH-1 were assessed by one-way ANOVA followed by Dunnett's multiple comparison test: *, $P < 0.05$; **, $P < 0.01$; ***, $P < 0.001$; ****, $P < 0.0001$. (D) Supernatants from JFH-1-, S512C-, and S686T-transfected cells were harvested at 72 h and assessed for the ability to mediate pH-dependent, CD81-independent membrane fusion. Supernatants were concentrated 10-fold by ultracentrifugation through a 20% sucrose cushion. Pellets were resuspended in buffer (10 mM Tricine-NaOH, 150 mM NaCl) and directly applied to the fusion assay. At time zero, fusion was initiated by acidifying the medium to pH 5.0 through addition of diluted HCl to the cuvette. The value for complete lipid mixing, which corresponds to 100% fluorescence, was obtained by adding 0.1% (vol/vol; final concentration) Triton X-100 to the suspension.

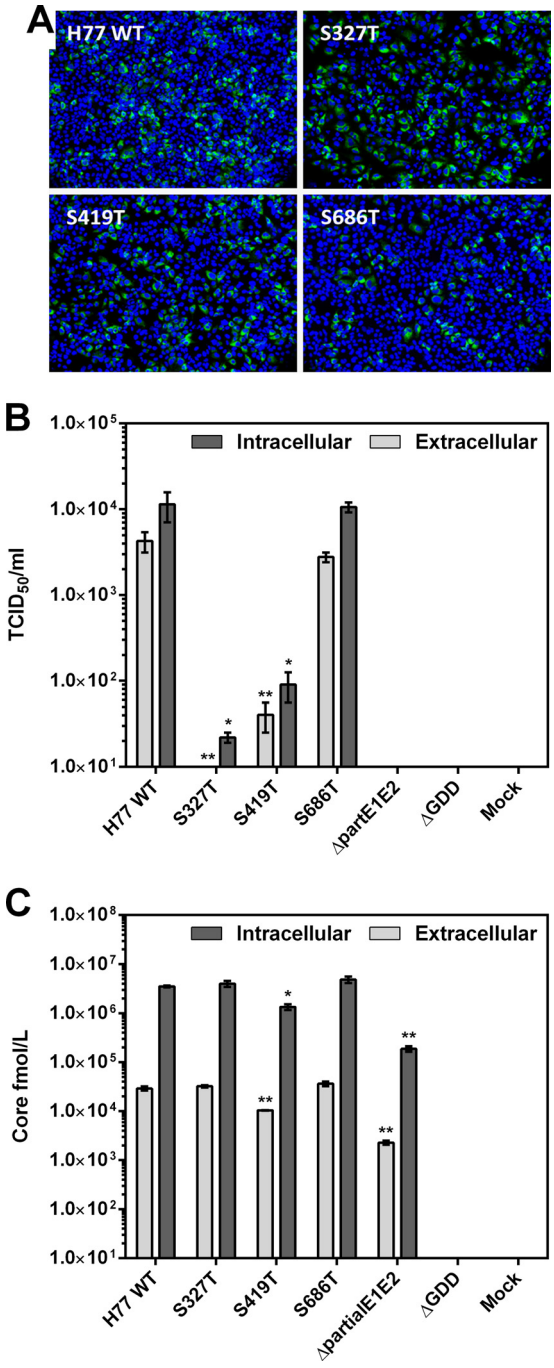

FIG 6 Impact of genetic background on transitional phenotypes. (A) As previously, viral replication was assessed via immunofluorescence staining. (B) The titers of infectious particles in both intracellular and extracellular fractions were determined at 72 h postelectroporation via $TCID_{50}$. The results presented are mean intracellular and extracellular $TCID_{50}$ values from two independent experiments; error bars show SEM. (C) The amount of core antigen (fmol/liter) in both intracellular and extracellular fractions was determined at 72 h postelectroporation via anti-core ELISA. The results are means from two independent experiments; error bars show SEM. Statistical significance of differences in both intracellular and extracellular HCVcc infectivity and amounts of core between individual mutants and H77 WT was assessed by one-way ANOVA followed by Dunnett's multiple comparison test: *, $P < 0.05$; **, $P < 0.01$; ***, $P < 0.001$; ****, $P < 0.0001$.

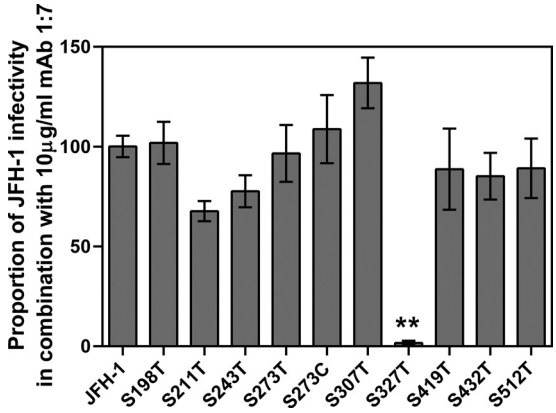

FIG 7 Sensitivity of transitional phenotypes to antibody-mediated neutralization. Neutralization sensitivity of authentic virions was assessed using the broadly neutralizing human MAb 1:7. Mixtures of 100 FFU and 200 FFU virus and 10 μg/ml of MAb 1:7 were used to assess sensitivity to neutralization, and assays were performed in triplicate. Values are normalized to the neutralization observed for WT JFH-1. Error bars indicate SEM. Differences in mean infectivity were assessed using unpaired *t* tests with the Bonferroni correction for multiple analyses. **, $P < 0.01$.

apparent from our viral sequence data analysis. Limitations restricting transitional phenotypes also act at the level of viral entry into target cells. Intergenotypic domain swapping experiments indicate that the stem region of E2, located at the C-terminal end of the protein, plays a major role in viral entry (15). We demonstrate that, in agreement with these data, intermediate phenotypes, occurring in the stem region of E2 and detectable at low frequencies in naturally circulating strains, can have a dramatic effect on the entry fitness of authentic viral particles bearing genotype 2a glycoproteins. Additionally, our data also identify mutations in E1, which negatively impact efficient entry of authentic virions bearing genotype 1a glycoproteins. These data suggest that restrictions against transitional intermediates can act at the level of viral entry to permissive cells and that these refractive effects are position dependent and isolate specific. Together, these data indicate that structural and functional restrictions exist at the level of virion assembly and target cell entry.

Our study surveyed the fitness cost of only a very limited proportion of possible mutations at highly conserved residues in the *E1E2* genes, encoding the envelope glycoproteins. A high proportion of randomly introduced mutations in viral genomes result in either lethal or deleterious phenotypes (46, 47). Thus, it is likely that intermediate phenotypes, occurring at conserved serine residues in viral proteins other than E1 and E2, may negatively impact additional aspects of the viral life cycle. Indeed, while codon switching in the NS5B polymerase is beyond the scope of this study, the RNA binding groove mutation S283T has been shown to confer resistance to all 2′-modified nucleoside inhibitors (NIs) in cell culture (48). This mutation immediately reverts in the absence of drug pressure. However, S283T results in a drastic decrease in viral fitness (49) and is consequently never seen in patients (48). Thus, while we did not identify any intermediates in E1E2 which negatively impact the RNA replication step of the viral life cycle, restrictions against S-S switching via intermediates in the NS5B polymerase are also apparent at the level of viral replication.

The interplay of multiple additional factors undoubtedly con-

tributes to restriction against fixation of intermediate phenotypes in globally sampled strains. HLA class I- and II-restricted T-cell responses will also represent a possible driving force underlying differential serine codon structures observed in multiple HCV lineages. However, knowledge of the HCV-infected host's HLA haplotype, which differs substantially between individuals and populations, would be required to validate this hypothesis. Additionally, increasing evidence indicates that genomic secondary structure elements are a common feature in RNA viruses (50–52). Consequently, constraints restricting viral genome mutability at conserved serine residues may also exist at the genomic level.

In conclusion, in this study we endeavored to replicate the highly complex interplay between virus and host, using multiple *in vitro* systems. However, these systems are highly artificial and cannot faithfully replicate the exact conditions which gave rise to the multiple ancient switches we observe in globally sampled strains. While the limitations of *in vitro* experimentation on laboratory strains allow only cautious extrapolation of putative mutational processes underlying S-S switching to globally circulating HCV isolates, our data indicate that switching can proceed through transitional intermediates and that differential structural, functional, and immunological constraints shape envelope glycoprotein evolution. Indeed, these data reveal that S-S codon-conversions represent the genomic relics of past purifying selection against less-fit intermediate phenotypes and also provide novel insight into the selection pressures that influence viral evolution, and fixation of mutations, at the global level. Broadly, our study provides a framework for combining community acquired genomic data and phylogenetic analyses with downstream phenotypic investigation, to identify restrictions on genome mutability. Ultimately, this framework could be applied to many medically important viral pathogens to define the barriers limiting the emergence of escape variants to candidate antivirals/vaccines, in addition to estimating evolutionary thresholds to viral zoonotic transmission to humans.

ACKNOWLEDGMENTS

We thank Takaji Wakita for plasmid pJFH-1, Charles Rice for the Huh7.5 cell line, MAb 9E10, and the H77/JFH-1 chimera, Arvind Patel for MAbs ALP98 and AP33, Jane McKeating for MAb 3/11, Mats A. A. Persson for MAb 1/7, Dennis Burton for MAbs AR3A, AR3B, and AR3C, Steven Foung for MAb CBH4G, and Francois Loïc Cosset for plasmid phCMV.

T.P. was supported by an ERC starting grant (VIRAFRONT). J.K.B. was funded by the Medical Research Council (grant G0801169) and the European Union (Health-F4-2012-305600 and MRTN-CT-2006-035599).

REFERENCES

1. **Shepard CW, Finelli L, Alter MJ.** 2005. Global epidemiology of hepatitis C virus infection. Lancet Infect. Dis. **5:**558–567. http://dx.doi.org/10.1016/S1473-3099(05)70216-4.
2. **Hoofnagle JH.** 2002. Course and outcome of hepatitis C. Hepatology **36:**S21–S29. http://dx.doi.org/10.1053/jhep.2002.36227.
3. **Simmonds P.** 2004. Genetic diversity and evolution of hepatitis C virus—15 years on. J. Gen. Virol. **85:**3173–3188. http://dx.doi.org/10.1099/vir.0.80401-0.
4. **Lindenbach BD, Rice CM.** 2005. Unravelling hepatitis C virus replication from genome to function. Nature **436:**933–938. http://dx.doi.org/10.1038/nature04077.
5. **Neumann AU, Lam NP, Dahari H, Gretch DR, Wiley TE, Layden TJ, Perelson AS.** 1998. Hepatitis C viral dynamics in vivo and the antiviral efficacy of interferon-alpha therapy. Science **282:**103–107. http://dx.doi.org/10.1126/science.282.5386.103.
6. **Martell M, Esteban JI, Quer J, Genesca J, Weiner A, Esteban R, Guardia J, Gomez J.** 1992. Hepatitis C virus (HCV) circulates as a population of different but closely related genomes: quasispecies nature of HCV genome distribution. J. Virol. **66:**3225–3229.
7. **Bukh J, Miller RH, Purcell RH.** 1995. Genetic heterogeneity of hepatitis C virus: quasispecies and genotypes. Semin. Liver Dis. **15:**41–63. http://dx.doi.org/10.1055/s-2007-1007262.
8. **Brown RJ, Tarr AW, McClure CP, Juttla VS, Tagiuri N, Irving WL, Ball JK.** 2007. Cross-genotype characterization of genetic diversity and molecular adaptation in hepatitis C virus envelope glycoprotein genes. J. Gen. Virol. **88:**458–469. http://dx.doi.org/10.1099/vir.0.82357-0.
9. **Brown RJP, Juttla VS, Tarr AW, Finnis R, Irving WL, Hemsley S, Flower DR, Borrow P, Ball JK.** 2005. Evolutionary dynamics of hepatitis C virus envelope genes during chronic infection. J. Gen. Virol. **86:**1931–1942. http://dx.doi.org/10.1099/vir.0.80957-0.
10. **Ray SC, Wang YM, Laeyendecker O, Ticehurst JR, Villano SA, Thomas DL.** 1999. Acute hepatitis C virus structural gene sequences as predictors of persistent viremia: hypervariable region 1 as a decoy. J. Virol. **73:**2938–2946.
11. **Sheridan I, Pybus OG, Holmes EC, Klenerman P.** 2004. High-resolution phylogenetic analysis of hepatitis C virus adaptation and its relationship to disease progression. J. Virol. **78:**3447–3454. http://dx.doi.org/10.1128/JVI.78.7.3447-3454.2004.
12. **von Hahn T, Yoon JC, Alter H, Rice CM, Rehermann B, Balfe P, McKeating JA.** 2007. Hepatitis C virus continuously escapes from neutralizing antibody and T-cell responses during chronic infection in vivo. Gastroenterology **132:**667–678. http://dx.doi.org/10.1053/j.gastro.2006.12.008.
13. **Logvinoff C, Major ME, Oldach D, Heyward S, Talal A, Balfe P, Feinstone SM, Alter H, Rice CM, McKeating JA.** 2004. Neutralizing antibody response during acute and chronic hepatitis C virus infection. Proc. Nat. Acad. Sci. U. S. A. **101:**10149–10154. http://dx.doi.org/10.1073/pnas.0403519101.
14. **Fafi-Kremer S, Fofana I, Soulier E, Carolla P, Meuleman P, Leroux-Roels G, Patel AH, Cosset FL, Pessaux P, Doffoel M, Wolf P, Stoll-Keller F, Baumert TF.** 2010. Viral entry and escape from antibody-mediated neutralization influence hepatitis C virus reinfection in liver transplantation. J. Exp. Med. **207:**2019–2031. http://dx.doi.org/10.1084/jem.20090766.
15. **Albecka A, Montserret R, Krey T, Tarr AW, Diesis E, Ball JK, Descamps V, Duverlie G, Rey F, Penin F, Dubuisson J.** 2011. Identification of new functional regions in hepatitis C virus envelope glycoprotein E2. J. Virol. **85:**1777–1792. http://dx.doi.org/10.1128/JVI.02170-10.
16. **Pietschmann T, Kaul A, Koutsoudakis G, Shavinskaya A, Kallis S, Steinmann E, Abid K, Negro F, Dreux M, Cosset FL, Bartenschlager R.** 2006. Construction and characterization of infectious intragenotypic and intergenotypic hepatitis C virus chimeras. Proc. Nat. Acad. Sci. U. S. A. **103:**7408–7413. http://dx.doi.org/10.1073/pnas.0504877103.
17. **Steinmann E, Penin F, Kallis S, Patel AH, Bartenschlager R, Pietschmann T.** 2007. Hepatitis C virus p7 protein is crucial for assembly and release of infectious virions. PLoS Pathog. **3:**e103. http://dx.doi.org/10.1371/journal.ppat.0030103.
18. **Helle F, Vieyres G, Elkrief L, Popescu CI, Wychowski C, Descamps V, Castelain S, Roingeard P, Duverlie G, Dubuisson J.** 2010. Role of N-linked glycans in the functions of hepatitis C virus envelope proteins incorporated into infectious virions. J. Virol. **84:**11905–11915. http://dx.doi.org/10.1128/JVI.01548-10.
19. **Pileri P, Uematsu Y, Campagnoli S, Galli G, Falugi F, Petracca R, Weiner AJ, Houghton M, Rosa D, Grandi G, Abrignani S.** 1998. Binding of hepatitis C virus to CD81. Science **282:**938–941. http://dx.doi.org/10.1126/science.282.5390.938.
20. **Scarselli E, Ansuini H, Cerino R, Roccasecca RM, Acali S, Filocamo G, Traboni C, Nicosia A, Cortese R, Vitelli A.** 2002. The human scavenger receptor class B type I is a novel candidate receptor for the hepatitis C virus. EMBO J. **21:**5017–5025. http://dx.doi.org/10.1093/emboj/cdf529.
21. **Evans MJ, von Hahn T, Tscherne DM, Syder AJ, Panis M, Wolk B, Hatziioannou T, McKeating JA, Bieniasz PD, Rice CM.** 2007. Claudin-1 is a hepatitis C virus co-receptor required for a late step in entry. Nature **446:**801–805. http://dx.doi.org/10.1038/nature05654.
22. **Ploss A, Evans MJ, Gaysinskaya VA, Panis M, You H, de Jong YP, Rice CM.** 2009. Human occludin is a hepatitis C virus entry factor required for infection of mouse cells. Nature **457:**882–886. http://dx.doi.org/10.1038/nature07684.

23. **Haid S, Pietschmann T, Pecheur EI.** 2009. Low pH-dependent hepatitis C virus membrane fusion depends on E2 integrity, target lipid composition, and density of virus particles. J. Biol. Chem. **284:**17657–17667. http://dx.doi.org/10.1074/jbc.M109.014647.
24. **Lavillette D, Bartosch B, Nourrisson D, Verney G, Cosset FL, Penin F, Pecheur EI.** 2006. Hepatitis C virus glycoproteins mediate low pH-dependent membrane fusion with liposomes. J. Biol. Chem. **281:**3909–3917. http://dx.doi.org/10.1074/jbc.M509747200.
25. **Averof M, Rokas A, Wolfe KH, Sharp PM.** 2000. Evidence for a high frequency of simultaneous double-nucleotide substitutions. Science **287:**1283–1286. http://dx.doi.org/10.1126/science.287.5456.1283.
26. **Tamura K, Peterson D, Peterson N, Stecher G, Nei M, Kumar S.** 2011. MEGA5: molecular evolutionary genetics analysis using maximum likelihood, evolutionary distance, and maximum parsimony methods. Mol. Biol. Evol. **28:**2731–2739. http://dx.doi.org/10.1093/molbev/msr121.
27. **Guindon S, Dufayard JF, Lefort V, Anisimova M, Hordijk W, Gascuel O.** 2010. New algorithms and methods to estimate maximum-likelihood phylogenies: assessing the performance of PhyML 3.0. Syst. Biol. **59:**307–321. http://dx.doi.org/10.1093/sysbio/syq010.
28. **Wakita T, Pietschmann T, Kato T, Date T, Miyamoto M, Zhao Z, Murthy K, Habermann A, Krausslich HG, Mizokami M, Bartenschlager R, Liang TJ.** 2005. Production of infectious hepatitis C virus in tissue culture from a cloned viral genome. Nat. Med. **11:**791–796. http://dx.doi.org/10.1038/nm1268.
29. **Bartosch B, Dubuisson J, Cosset FL.** 2003. Infectious hepatitis C virus pseudo-particles containing functional E1-E2 envelope protein complexes. J. Exp. Med. **197:**633–642. http://dx.doi.org/10.1084/jem.20021756.
30. **Flint M, Maidens C, Loomis-Price LD, Shotton C, Dubuisson J, Monk P, Higginbottom A, Levy S, McKeating JA.** 1999. Characterization of hepatitis C virus E2 glycoprotein interaction with a putative cellular receptor, CD81. J. Virol. **73:**6235–6244.
31. **Lindenbach BD, Evans MJ, Syder AJ, Wolk B, Tellinghuisen TL, Liu CC, Maruyama T, Hynes RO, Burton DR, McKeating JA, Rice CM.** 2005. Complete replication of hepatitis C virus in cell culture. Science **309:**623–626. http://dx.doi.org/10.1126/science.1114016.
32. **Reed LJ, Muench H.** 1938. A simple method of estimating fifty per cent endpoints. Am. J. Hyg. **24:**493–497.
33. **Goffard A, Callens N, Bartosch B, Wychowski C, Cosset FL, Montpellier C, Dubuisson J.** 2005. Role of N-linked glycans in the functions of hepatitis C virus envelope glycoproteins. J. Virol. **79:**8400–8409. http://dx.doi.org/10.1128/JVI.79.13.8400-8409.2005.
34. **Helle F, Goffard A, Morel V, Duverlie G, McKeating J, Keck Z-Y, Foung S, Penin F, Dubuisson J, Voisset C.** 2007. The neutralizing activity of anti-hepatitis C virus antibodies is modulated by specific glycans on the E2 envelope protein. J. Virol. **81:**8101–8111. http://dx.doi.org/10.1128/JVI.00127-07.
35. **Johansson DX, Voisset C, Tarr AW, Aung M, Ball JK, Dubuisson J, Persson MAA.** 2007. Human combinatorial libraries yield rare antibodies that broadly neutralize hepatitis C virus. Proc. Nat. Acad. Sci. U. S. A. **104:**16269–16274. http://dx.doi.org/10.1073/pnas.0705522104.
36. **Wahid A, Helle F, Descamps V, Duverlie G, Penin F, Dubuisson J.** 2013. Disulfide bonds in hepatitis C virus glycoprotein E1 control the assembly and entry functions of E2 glycoprotein. J. Virol. **87:**1605–1617. http://dx.doi.org/10.1128/JVI.02659-12.
37. **Brown RJ, Hudson N, Wilson G, Rehman SU, Jabbari S, Hu K, Tarr AW, Borrow P, Joyce M, Lewis J, Zhu LF, Law M, Kneteman N, Tyrrell DL, McKeating JA, Ball JK.** 2012. Hepatitis C virus envelope glycoprotein fitness defines virus population composition following transmission to a new host. J. Virol. **86:**11956–11966. http://dx.doi.org/10.1128/JVI.01079-12.
38. **Giang E, Dorner M, Prentoe JC, Dreux M, Evans MJ, Bukh J, Rice CM, Ploss A, Burton DR, Law M.** 2012. Human broadly neutralizing antibodies to the envelope glycoprotein complex of hepatitis C virus. Proc. Nat. Acad. Sci. U. S. A. **109:**6205–6210. http://dx.doi.org/10.1073/pnas.1114927109.
39. **Keck ZY, Xia J, Wang Y, Wang W, Krey T, Prentoe J, Carlsen T, Li AY, Patel AH, Lemon SM, Bukh J, Rey FA, Foung SK.** 2012. Human monoclonal antibodies to a novel cluster of conformational epitopes on HCV E2 with resistance to neutralization escape in a genotype 2a isolate. PLoS Pathog. **8:**e1002653. http://dx.doi.org/10.1371/journal.ppat.1002653.
40. **Law M, Maruyama T, Lewis J, Giang E, Tarr AW, Stamataki Z, Gastaminza P, Chisari FV, Jones IM, Fox RI, Ball JK, McKeating JA, Kneteman NM, Burton DR.** 2008. Broadly neutralizing antibodies protect against hepatitis C virus quasispecies challenge. Nat. Med. **14:**25–27. http://dx.doi.org/10.1038/nm1698.
41. **Dorner M, Horwitz JA, Robbins JB, Barry WT, Feng Q, Mu K, Jones CT, Schoggins JW, Catanese MT, Burton DR, Law M, Rice CM, Ploss A.** 2011. A genetically humanized mouse model for hepatitis C virus infection. Nature **474:**208–211. http://dx.doi.org/10.1038/nature10168.
42. **Bankwitz D, Steinmann E, Bitzegeio J, Ciesek S, Friesland M, Herrmann E, Zeisel MB, Baumert TF, Keck ZY, Foung SK, Pecheur EI, Pietschmann T.** 2010. Hepatitis C virus hypervariable region 1 modulates receptor interactions, conceals the CD81 binding site, and protects conserved neutralizing epitopes. J. Virol. **84:**5751–5763. http://dx.doi.org/10.1128/JVI.02200-09.
43. **Van Valen L.** 1973. A new evolutionary law. Evol. Theory **1:**1–30.
44. **Krey T, d'Alayer J, Kikuti CM, Saulnier A, Damier-Piolle L, Petitpas I, Johansson DX, Tawar RG, Baron B, Robert B, England P, Persson MA, Martin A, Rey FA.** 2010. The disulfide bonds in glycoprotein E2 of hepatitis C virus reveal the tertiary organization of the molecule. PLoS Pathog. **6:**e1000762. http://dx.doi.org/10.1371/journal.ppat.1000762.
45. **Cocquerel L, Wychowski C, Minner F, Penin F, Dubuisson J.** 2000. Charged residues in the transmembrane domains of hepatitis C virus glycoproteins play a major role in the processing, subcellular localization, and assembly of these envelope proteins. J. Virol. **74:**3623–3633. http://dx.doi.org/10.1128/JVI.74.8.3623-3633.2000.
46. **Sanjuan R.** 2010. Mutational fitness effects in RNA and single-stranded DNA viruses: common patterns revealed by site-directed mutagenesis studies. Philos. Trans. R. Soc. Lond. B Biol. Sci. **365:**1975–1982. http://dx.doi.org/10.1098/rstb.2010.0063.
47. **Sanjuan R, Moya A, Elena SF.** 2004. The distribution of fitness effects caused by single-nucleotide substitutions in an RNA virus. Proc. Nat. Acad. Sci. U. S. A. **101:**8396–8401. http://dx.doi.org/10.1073/pnas.0400146101.
48. **Bartenschlager R, Lohmann V, Penin F.** 2013. The molecular and structural basis of advanced antiviral therapy for hepatitis C virus infection. Nat. Rev. Microbiol. **11:**482–496. http://dx.doi.org/10.1038/nrmicro3046.
49. **Dutartre H, Bussetta C, Boretto J, Canard B.** 2006. General catalytic deficiency of hepatitis C virus RNA polymerase with an S282T mutation and mutually exclusive resistance towards 2′-modified nucleotide analogues. Antimicrob. Agents Chemother. **50:**4161–4169. http://dx.doi.org/10.1128/AAC.00433-06.
50. **Davis M, Sagan SM, Pezacki JP, Evans DJ, Simmonds P.** 2008. Bioinformatic and physical characterizations of genome-scale ordered RNA structure in mammalian RNA viruses. J. Virol. **82:**11824–11836. http://dx.doi.org/10.1128/JVI.01078-08.
51. **Simmonds P, Tuplin A, Evans DJ.** 2004. Detection of genome-scale ordered RNA structure (GORS) in genomes of positive-stranded RNA viruses: Implications for virus evolution and host persistence. RNA **10:**1337–1351. http://dx.doi.org/10.1261/rna.7640104.
52. **Watts JM, Dang KK, Gorelick RJ, Leonard CW, Bess JW, Jr, Swanstrom R, Burch CL, Weeks KM.** 2009. Architecture and secondary structure of an entire HIV-1 RNA genome. Nature **460:**711–716. http://dx.doi.org/10.1038/nature08237.